Dalton Transactions

An international journal of inorganic chemistry

This article can be cited before page numbers have been issued, to do this please use: J. Li, C. Wei, D. Guo, C. Wang, Y. Han, G. He, J. Zhang, X. Huang and C. Hu, *Dalton Trans.*, 2020, DOI: 10.1039/D0DT03015E.

ROYAL SOCIETY OF CHEMISTRY

rsc.li/dalton

ROYAL SOCIETY OF CHEMISTRY
View Article Online
DOI: 10.1039/D0DT03015E

Journal Name

Article

Inorganic-Organic Hybrid Polyoxovanadates Based on $[V_4O_{12}]^{4-}$ or $[VO_3]_2^{2-}$ Clusters: Controllable Synthesis, Crystal Structures and Catalytic Properties in Selective Oxidation of Sulfides

Received 00th January 20xx,
Accepted 00th January 20xx

DOI: 10.1039/x0xx00000x

www.rsc.org/

Jikun Li,*[a,b] Chuanping Wei,[a] Daigaojie Guo,[a] Congcong Wang,[a] Yinfeng Han,[a] Guofang He,[a] Jianping Zhang,[a] Xianqiang Huang,[c] and Changwen Hu*[b]

By rationally controlling of the hydrothermal conditions, three new inorganic-organic hybrid polyoxovanadates (POVs) $[Ni_2(1\text{-vIM})_7H_2O][V_4O_{12}]\cdot H_2O$ **(1)**, $[Cu_2(1\text{-vIM})_8][V_4O_{12}]\cdot H_2O$ **(2)** and $[Co(1\text{-vIM})H_2O][VO_3]_2$ **(3)** (1-vIM = 1-vinylimidazole) have been synthesized and thoroughly characterized by single X-ray diffraction (SXRD), powder X-ray diffraction (PXRD), infrared spectroscopy (FT-IR), and elemental analyses (EA). Interestingly, complexes **1** and **2** have similar structures including $[V_4O_{12}]^{4-}$ clusters, complex **3** however, was isolated as a structure including $[VO_3]_2^{2-}$ cluster under a different synthetic condition compared with that of **1** and **2**. Both complexes **1** and **2** display an interesting 3D supramolecular structure and complex **3** shows a 2D two parallel network supramolecular structure linked by a $[Co_2O_2]$ unit due to the different coordination environments of the central metals. Three inorganic-organic hybrid POVs as heterogeneous catalysts are active in the selective oxidation of sulfides to produce sulfoxides or sulfones with high conversion and high selectivity (up to 99.5% for sulfoxides and 98.5% for sulfones respectively catalyzed by **1**). Complex **1** is also used as catalyst in the oxidative CEES (2-chloroethyl ethyl sulfide, a sulfur mustard simulant) abatement with high activity and selectivity toward corresponding sulfoxide. Moreover, complex **1** can be reused for at least three times in sulfoxidation reactions without losing its activity.

Introduction

As a class of multinuclear complexes, polyoxometalates (POMs) have some excellent physicochemical properties, such as the ability to accept electrons and protons reversibly, variability in cluster structures or size and high chemical stability, which have broad their application prospects in the fields of catalysis, materials, biology and energy, etc.[1] Polyoxovanadates (POVs) is a unique branch of POMs due to their diverse structures, multiple valence states and variable coordination configurations. All these properties make POVs a preferred building block for the design and assembly of POVs-based inorganic-organic hybrid materials.[2] Many factors, such as initial reactants along with their stoichiometry ratios, pH value, temperature and solvents etc, can influence the ultimate structures of inorganic-organic hybrid POVs.[3] As for POVS, the structure of $[V_xO_y]^{n-}$ ranges from monomeric $[VO_4]^{3-}$ unit to polymeric $[V_2O_7]^{4-}$, $[V_4O_{12}]^{4-}$ and $[V_6O_{18}]^{6-}$ *etc*, from $[VO_3]_n^{n-}$ chains to $[V_xO_y]^{n-}$ networks.[4] Compared with other properties, only a few research focused on catalysis of inorganic-organic hybrid POVs.[5] It is worth mentioning that the introduction of transition-metal species into the POVs systems usually led to heterogenous catalysts in various organic reactions with excellent performence. Up to now, some inorganic-organic hybrid POVs, such as $M(HAep)_2(VO_3)_4$ (M = Co, Ni, Cu; Aep = 1-(2-aminoethl)piperazine),[6] $[\{CoNi(H_2O)_2(Bpe)_2\}(V_4O_{12})]\cdot 4H_2O\cdot Bpe$,[7] $[\{Ag(Bpy)\}_4(V_4O_{12})]\cdot 2H_2O$, $[\{Ag(Dpa)\}_4(V_4O_{12})]\cdot 4H_2O$ and $\{Ag_4(2\text{-}Pzc)_2\}(V_2O_6)$ (Bpy = 4,4'-bipyridine; Dpa = 1,2-bis(4-pyridyl)-ethane; Pzc = pyrazinecarboxylate),[8] $[Ag(Bbi)]\{Ag(Bbi)\}_4\{Ag_3(V_4O_{12})_2\}]\cdot 2H_2O$ (Bbi = 1,4-bis(N-imidazolyl)butane),[9] $Mn(Bpy)(V_4O_{11})(Bpy)$,[10] $[Co_2L_{0.5}V_4O_{12}]\cdot 3DMF\cdot 5H_2O$ (L = resorcin[4]arene),[11] $[Co(bib)]\{V_2O_6\}$ and $[Ni(en)(bib)]\{V_2O_6\}\cdot 2H_2O$ (bib = 1,4-bis(1H-imidazoly-1-yl)benzene), en = ethylenediamine)[12] etc., have been used in the catalytic field of the oxidation of sulfides, the cyanosilylation of aldehydes with trimethylsilyl cyanide, the decomposition of methylene blue, splitting of water, degradation of pollutants, and the cycloaddition of CO_2 with epoxides.

As important high value added products, sulfoxides and sulfones are commonly used as chiral auxiliaries,[13] oxo-transfer reagents[14] and versatile building blocks for the construction of chemical and biological molecules.[15] The desirable route to obtain sulfoxides and sulfones is the selective oxidation of

---

[a.] *College of Chemistry and Chemical Engineering, Taishan University, Tai'an, 271021, Shandong, P. R. China.*
[b.] *Key Laboratory of Cluster Science Ministry of Education, Beijing Key Laboratory of Photoelectronic/Electrophotonic, School of Chemistry, Beijing Institute of Technology, Beijing, 100081 P.R. China.*
[c.] *Shandong Provincial Key Laboratory of Chemical Energy Storage and Novel Cell Technology, School of Chemistry & Chemical Engineering, Liaocheng University, Liaocheng, 252059, Shandong, P. R. China.*
E-mail address: lijk0212@163.com, cwhu@bit.edu.cn.

Electronic Supplementary Information (ESI) available: characterization data, copies of IR and PXRD spectra and single crystal data. See DOI: 10.1039/x0xx00000x

View Article Online
DOI: 10.1039/D0DT03015F

sulfides using environmental economical oxidant to replace the traditional stoichiometric oxidants.[16-19] Nevertheless, only a few procedures are suitable for switchable synthesis of sulfoxides or sulfones *via* the oxidation reaction of sulfides with the same oxidant.[20-23] The vanadium peroxides are effective oxidants either stoichiometric or catalytic using H_2O_2 as the terminal environmentally friendly oxidant in many oxidative transformations including sulfoxidation process. Therefore, exploring new synthetic methods for more stable, highly active and selective catalysts based on vanadium clusters in sulfoxidation transformation is essential.

Imidazoles, in general, are important in biomolecules,[24] and pharmaceutical applications[25] etc. The substituent at the heteroatom blocks up the possibility for tautomerism type of the original imidazole and the non-coordinated nitrogen atom remains a site of high tendency to coordinate to metal centers.[26] In our previous works, 1-methylimidazole,[27] 1-ethylimidazole,[28] 1-propylimidazole and 1-isopropylimidazole[29] have been used as N-donor ligands to synthesize inorganic-organic hybrid POVs and their catalytic properties in oxidation of sulfides and alcohols, epoxidation of olefin and Chan-Lam reaction were also studied. To further investigate the controlling synthetic method and advance our research in the field of oxidative catalytic activity of POVs based catalysts,[30] herein, we synthesized three new inorganic-organic hybrid POVs complexes $[Ni_2(1\text{-vIM})_7H_2O][V_4O_{12}]\cdot H_2O$ **(1)**, $[Cu_2(1\text{-vIM})_8][V_4O_{12}]\cdot H_2O$ **(2)** and $[Co(1\text{-vIM})H_2O][VO_3]_2$ **(3)** by selecting 1-vinylimidazole (1-vIM) as the N-donor ligand to assemble with ammonium metavanadate and different metal ions under hydrothermal conditions. Complexes **1**-**3** have been thoroughly characterized by SXRD, PXRD, FT-IR and EA. In order to compare the catalytic activity, complex $[Co_4(1\text{-vIM})_{14}][V_4O_{12}]_2\cdot 6H_2O$ **(4)** was also synthesized according to our previous work.[31] Further, the catalytic activity of complexes **1**-**4** as heterogeneous catalysts were probed in the selective oxidatition of sulfides using H_2O_2 as oxidant. By optimizing the reaction conditions, we can obtain sulfoxides or sulfones with high conversion and selectivity respectively.

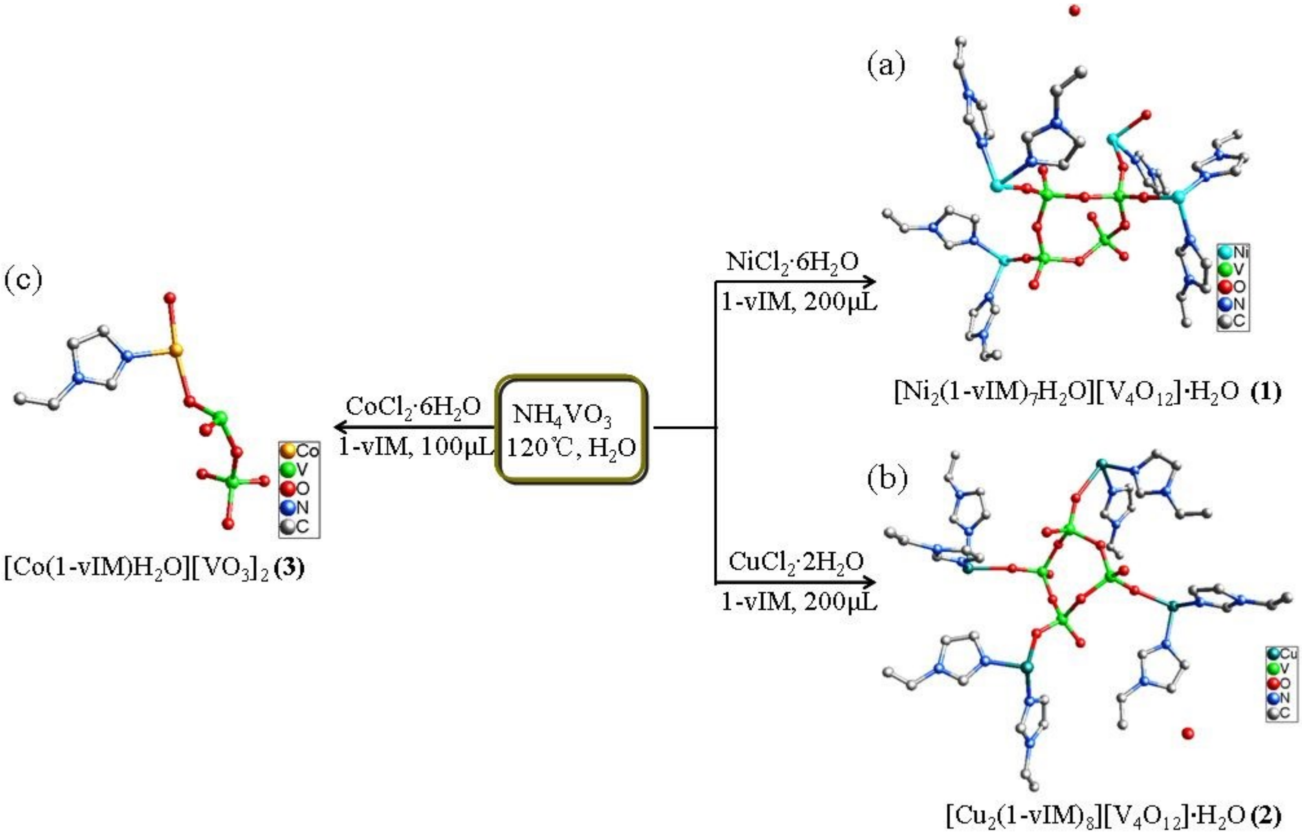

Scheme 1. The controlling synthesis of complexes **1**-**3**. All hydrogen atoms are omitted for clarity.

Results and discussion

Syntheses

To further explore the control toward the formation of the various architectures of inorganic-organic hybrid POVs with potential applications, we chose NH_4VO_3 as vanadium source to react with metal(II) chlorides ($NiCl_2\cdot 6H_2O$, $CuCl_2\cdot 2H_2O$ and $CoCl_2\cdot 6H_2O$) and 1-vIM under hydrothermal conditions (Scheme 1). As expected, similar structures of inorganic-organic hybrid POVs based on $[V_4O_{12}]^{4-}$ unit were obtained under the same reaction conditions except the metal(II) ions for complexes **1**, **2** and **4** (Complex $[Co_4(1\text{-vIM})_{14}][V_4O_{12}]_2\cdot 6H_2O$ (**4**) was reported in our previous work[31]). Different from complexes **1** and **2**, the crystal quality of complex **4** is poor. When we try to improve the

View Article Online
DOI: 10.1039/D0DT03015E

crystal quality of **4** and adjust the synthetic conditions with reducing both $CoCl_2·6H_2O$ and 1-vIM to half amounts, a new complex **3** based on $[VO_3]_2^{2-}$ unit was isolated successfully.

Structural analysis of complex $[Ni_2(1\text{-vIM})_7H_2O][V_4O_{12}]·H_2O$ (1)

According to the coordination environment of the central nickel atoms, the molecular formula of **1** should be written as $[Ni_{0.5}(1\text{-vIM})_2]_3[Ni_{0.5}(1\text{-vIM})H_2O][V_4O_{12}]·H_2O$. As shown in Figure 1, the SXRD analysis reveals that **1** consists of four Ni^{2+} cations (the atom occupancy rate of all Ni atoms in the crystal data is 0.5), one $[V_4O_{12}]^{4-}$ anion cluster, and seven 1-vIM ligands. All four Ni atoms in **1** are six-coordination in an octahedral geometry. The coordination atoms of Ni(1), Ni(3) and Ni(4) include two O atoms come from two $[VO_4]$ tetrahedron and four N atoms from four 1-vIM ligands around the central nickel atom. The six-coordinated Ni(2) center is ligated by two O atoms come from two $[VO_4]$ tetrahedron, four N atoms from four 1-vIM ligands and two O atoms from two water molecules. All V atoms in $[V_4O_{12}]^{4-}$ anion cluster possess a distorted $[VO_4]$ tetrahedral geometry. Among them, the coordination atoms of V(1) include two bridging O atoms from two adjacent $[VO_4]$ tetrahedrons and two bridging O atoms from $[Ni(1)N_4O_2]$ and $[Ni(2)N_2O_4]$ octahedrons, respectively. The coordination environments of V(2) and V(3) are same and achieved by two bridging O atoms from two adjacent $[VO_4]$ tetrahedrons, one bridging O atoms from $[Ni(3)N_4O_2]$ for V(2) and $[Ni(4)N_4O_2]$ for V(3) octahedrons and a terminal O atom. The coordination environment of V(4) however, includes two bridging O atoms from two adjacent $[VO_4]$ tetrahedrons and two terminal O atoms.

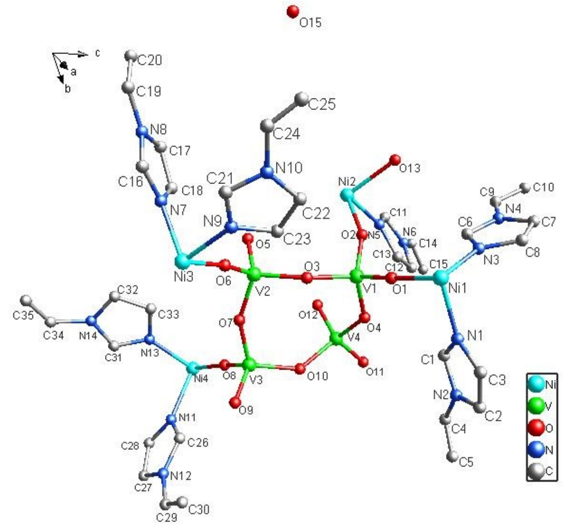

Figure 1. The crystal structure of complex **1**. All hydrogen atoms are omitted for clarity.

Complex **1** displays an interesting 3D supramolecular structure. Such an intriguing structure can be described in the following steps: first, four adjacent $[VO_4]$ tetrahedrons are connected by the corner-sharing O atoms to form $[V_4O_{12}]^{4-}$ clusters and the alternate $[V(1)O_4]$ and $[V(3)O_4]$ tetrahedrons of each $[V_4O_{12}]^{4-}$ cluster are linked by two $[Ni(1\text{-vIM})_4]^{2+}$ subunits, giving rise to a 1D chain structure along the [110] plane (Figure 2(a)); then, the $[V(1)O_4]$ tetrahedron provides one of its terminal O atoms O(2) to coordinate with $[Ni(1\text{-vIM})_2(H_2O)_2]^{2+}$ subunit connecting the adjacent 1D chain to a 2D network parallel to the [110] plane (Figure 2(b)); at last, the $[V(2)O_4]$ tetrahedron uses one of its terminal O atoms to connect with $[Ni(1\text{-vIM})_4]^{2+}$ subunit linking the 2D network to a 3D supramolecular structure (Figure 2(c)).

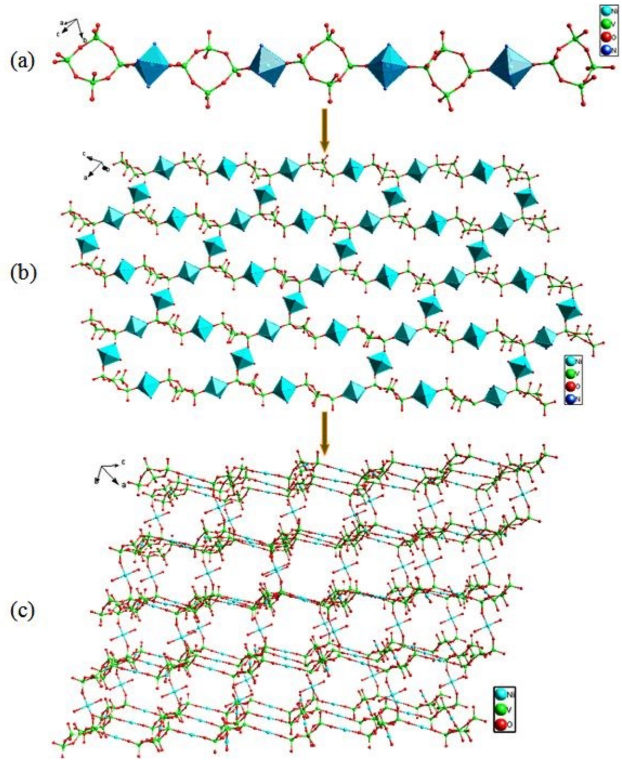

Figure 2. (a) The 1D chain structure in **1**. (b) The 2D network in **1**. (c) The 3D supramolecular structure of **1**. Color code: $[NiN_4O_2]$ octahedron, sky blue. All hydrogen and carbon atoms are omitted for clarity and nitrogen atoms in (c) are also omitted.

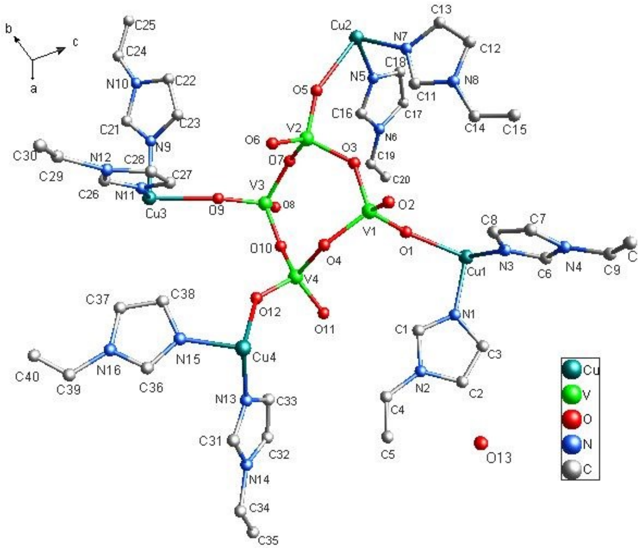

Figure 3. The crystal structure of complex **2**. All hydrogen atoms are omitted for clarity.

View Article Online
DOI: 10.1039/D0DT03015E

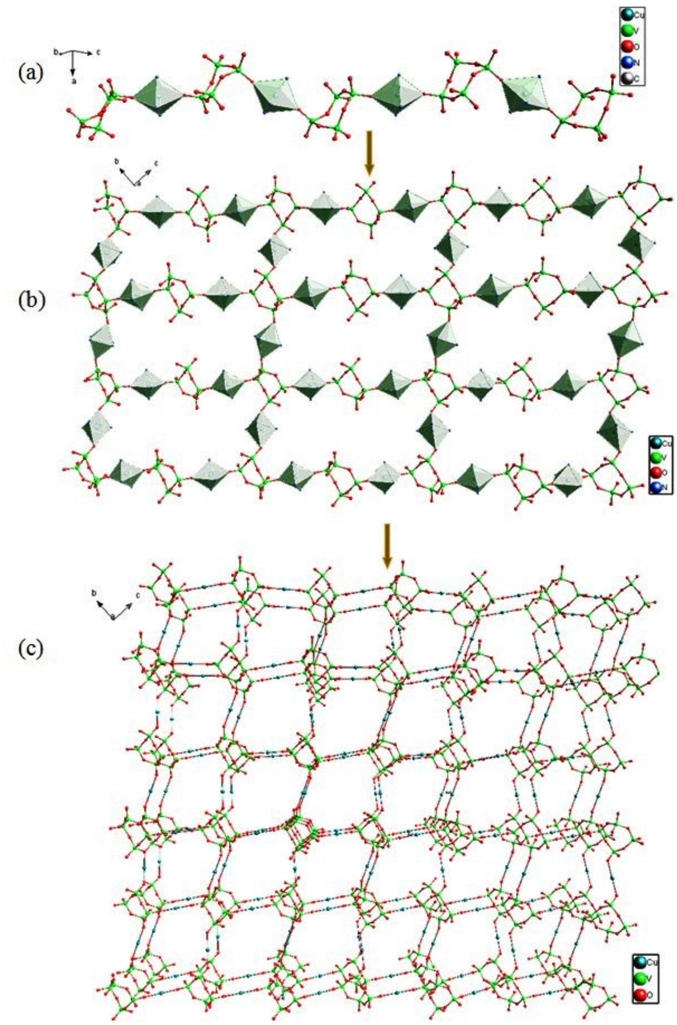

Figure 4. (a) The 1D zigzag chain structure in **2**. (b) The 2D network in **2**. (c) The 3D supramolecular structure of **2**. Color code: [CuN_4O_2] octahedron, light green. All hydrogen and carbon atoms are omitted for clarity and nitrogen atoms in (c) are also omitted.

Structural analysis of complex [Cu_2(1-vIM)$_8$][V_4O_{12}]·H_2O (2)

According to the coordination environment of the central copper atoms, the molecular formula of **2** should be written as [$Cu_{0.5}$(1-vIM)$_2$]$_4$[V_4O_{12}]·H_2O. Although complexes **1** and **2** have the same [V_4O_{12}]$^{4-}$ anion cluster, the coordination environments of [VO_4] tetrahedrons are very different. In **1**, the [V(1)O_4] tetrahedron coordinate to [Ni(1-vIM)$_4$]$^{2+}$ and [Ni(1-vIM)$_2$(H_2O)$_2$]$^{2+}$ subunits respectively, and the [V(4)O_4] tetrahedron is free. As shown in Figure 3, in **2** however, each [VO_4] tetrahedron in [V_4O_{12}]$^{4-}$ cluster coordinate to one [Cu(1-vIM)$_4$]$^{2+}$ subunit respectively. The alternate [V(1)O_4] and [V(3)O_4] tetrahedrons of each [V_4O_{12}]$^{4-}$ cluster coordinate to two [Cu(1-vIM)$_4$]$^{2+}$ subunits, giving rise to a 1D zigzag chain structure along the crystallographic *c*-axis (Figure 4(a)); there are two directions of the [V_4O_{12}]$^{4-}$ pseudo planes in the 1D zigzag chain structure and through one direction of the [V_4O_{12}]$^{4-}$ pseudo plane, the [V(1)O_4] and [V(4)O_4] coordinates to [Cu(1-vIM)$_4$]$^{2+}$ subunits respectively connecting the adjacent 1D zigzag chains to a 2D network parallel to the *bc* plane (Figure 4(b)); at last, through another direction of the [V_4O_{12}]$^{4-}$ pseudo plane, the [V(1)O_4] and [V(4)O_4] connects with [Cu(1-vIM)$_4$]$^{2+}$ subunits linking the above 2D network to a 3D supramolecular structure (Figure 4(c)).

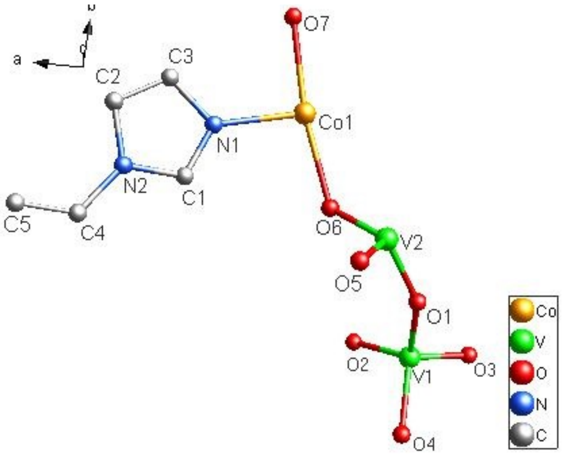

Figure 5. The crystal structure of complex **3**. All hydrogen atoms are omitted for clarity.

Structural analysis of complex [Co(1-vIM)H_2O][VO_3]$_2$ (3)

The structure analyses show that complexes [Co_4(1-vIM)$_{14}$][V_4O_{12}]$_2$·6H_2O **(4)** (Supporting Information Figure S11)[31] and [$Ni_{0.5}$(1-vIM)$_2$]$_3$[$Ni_{0.5}$(1-vIM)H_2O][V_4O_{12}]·H_2O **(1)** are isostructural and crystallize in the triclinic space group *P-1*, with very similar cell parameters. Yet, the crystal quality of **4** is poor. When we try to improve its crystal quality by adjusting the synthetic conditions, a new complex **3** based on [VO_3]$_2^{2-}$ unit was obtained.

As shown in Figure 5, the structural formula of **3** is [Co(1-vIM)H_2O][VO_3]$_2$, in which there are two crystallographically independent vanadium atoms with tetrahedral coordination environments. [VO_4] tetrahedrons in **3** are linked to each other through two of their vertex. This joint, gives rise to [VO_3]$_n^{n-}$ chains along the crystallographic *b*-axis (Figure 6(a)). The [V(1)O_4] and [V(2)O_4] tetrahedrons using their other two vertex coordinate to [Co(1-vIM)H_2O]$^{2-}$ subunits respectively, joining the adjacent [VO_3]$_n^{n-}$ chains together and forming a 2D network parallel to *bc* plane (Figure 6(b)). Interestingly, a [Co_2O_2] square plane structure unit (Figure S1) is formed via a bridging O(2) atom derived from the [V(1)O_4] tetrahedron coordinating to two [Co(1-vIM)H_2O]$^{2-}$ simultaneously. Through the [Co_2O_2] unit another 2D network parallel to the previous network is formed by joining the [VO_3]$_n^{n-}$ chains together (Figure 6(c)). This structure is relatively rare in the reported hybrid POVs complexes.

The selected bond lengths and angles are listed in Table S2. The bond lengths of V-O, V=O and angles of V-O-V in [V_4O_{12}]$^{4-}$ clusters of **1**, **2** and [VO_3]$_2^{2-}$ cluster of **3** are approximative with the similar structures reported previously.[32-34] The bond valence sum (BVS) calculations show that the oxidation states of all vanadium atoms are +V (Table S1), which are in good agreement with the charge balance of complexes **1**-**3**.

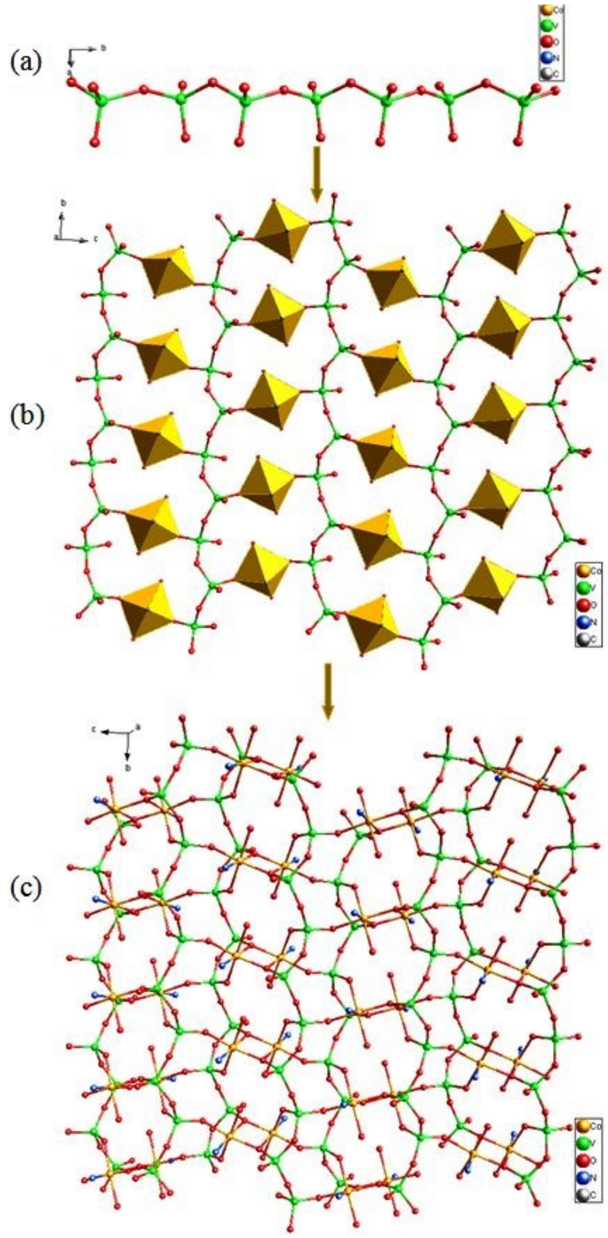

Figure 6. (a) The 1D $[VO_3]_n^{n-}$chain structure in **3**. (b) The 2D network in **3**. (c) Two parallel networks of **3**. Color code: $[CoNO_5]$ octahedron, gold. All hydrogen and carbon atoms are omitted for clarity.

PXRD and FT-IR spectra

The simulated and experimental PXRD patterns of three hybrid POVs complexes **1**-**3** are shown in Figures S6-S8. The diffraction peak positions of the experimental PXRD patterns of **1**-**3** are in good agreement with the simulated patterns from single crystal analysis, which indicate that the phase purity of bulk powders is satisfactory.

As shown in Figures S2-S4, the FT-IR spectra for complexes **1**-**3** can afford some valuable information for the investigation of POVs. Especially, the 400-1000 cm^{-1} region is worthy of careful determination, where M-O$_t$ (terminal oxygen atoms) and M-O$_b$ (bridging oxygen atoms) can be found. The V=O$_t$ stretching vibrations appear at 930, 925 and 916 cm^{-1} for **1**, **2** and **3** respectively. The absorption bands at 797, 655 and 594 cm^{-1} for **1**, 788, 654 and 600 cm^{-1} for **2** and 877 cm^{-1} 788 cm^{-1} and 640 cm^{-1} for **3** can be attributed to the bridging V-O-V or M-O-V stretching vibrations.[35] The apparent stretch absorption bands from 1650 cm^{-1} to 1510 cm^{-1} are assigned to C=C and C=N (1-vIM ligand).[36] Moreover, the absorption bands of coordinated and free water molecules in complexes **1**-**3** can be positioned at around 3300–3500 cm^{-1}.[37]

View Article Online
DOI: 10.1039/D0DT03015F

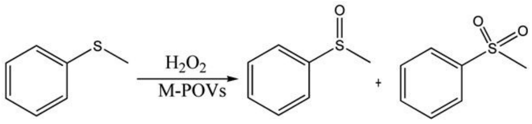

Scheme 2. Conversion of methyl phenyl sulfide to sulfoxide and sulfone catalyzed by M-POVs.

Table 1. Conversion of methyl phenyl sulfide to sulfoxide with different catalysts or without catalyst.[a]

Catalysts	Conv.(%)	Sele.(%)[b]	Reaction system
No	12.6	100	-
$[VO(1\text{-}vIM)_4]_2V_4O_{12}\cdot 6H_2O$[c]	>99	90.5	homogeneous
$Ni(1\text{-}vIM)_4Cl_2$[d]	28.2	100	heterogeneous
1	98.6	98.7	heterogeneous
2	98.8	96.5	heterogeneous
3	91.5	98.5	heterogeneous
4	98.2	96.8	heterogeneous

[a]methyl phenyl sulfide (0.25 mmol, 1 equiv.), catalyst (8.75 μmol, 3.5 mol%), 30% aq H_2O_2 (0.3 mmol, 1.2 equiv.), 45 °C, ethanol (1 mL), 4 h. [b]Selectivity to methyl phenyl sulfoxide. The byproduct is sulfone determined by GC-MS. [c]V content equivalent to **1**. [d]Ni content equivalent to **1**.

Catalytic Activities of Hybrid POVs in Sulfoxidation Reaction

The methyl phenyl sulfide was selected as a model substrate in sulfoxidation reaction to evaluate the catalytic activities of complexes **1**-**4** (Scheme 2). All catalysts were activated with two equivalent H_2O_2 (mole ratio) by stirring them in ethanol at 45 °C for 20 min before using. After the activation process, they were separated from ethanol and dried at ambient conditions for use. After much experimentation on optimizing solvent, amounts of catalyst and oxidant, temperature and the reaction time, the high conversion of sulfide and selectivity toward corresponding sulfoxide were reached under optimized conditions. As shown in Table 1, complexes **1**-**4** all can efficiently catalyze the oxidation of methyl phenyl sulfide to methyl phenyl sulfoxide with the conversion of 91.5%-98.8% and selectivity of 96.5%-98.7%. Among them, complexes **1**, **2** and **4** showed higher activity than complex **3** under optimized conditions. Given the similar coordination environments of Ni^{2+}, Cu^{2+} and Co^{2+} in complexes **1**-**4**, the different catalytic performance may be ascribed to the different vanadate units in complex **3** ($[VO_3]_2^{2-}$) compared with complexes **1**, **2** and **4** ($[V_4O_{12}]^{4-}$).

View Article Online
DOI: 10.1039/D0DT03045E

Due to the similar catalytic activity of complexes **1**, **2** and **4** and the higher yield, complex **1** was selected as the catalyst for further investigation in sulfoxidation reactions. To probe the role of each active center of complex **1** in the selective oxidation of sulfide toward sulfoxide, we further studied the avtivity of Ni(1-vIM)$_4$Cl$_2$ (Figure S10) and [VO(1-vIM)$_4$]$_2$V$_4$O$_{12}$·6H$_2$O.[38] As shown in Table 1, low conversion of sulfide (28.2%) and prominent selectivity toward corresponding sulfoxide (100%) were achieved when using Ni(1-vIM)$_4$Cl$_2$ as catalyst. When [VO(1-vIM)$_4$]$_2$V$_4$O$_{12}$·6H$_2$O was used as catalyst however, the conversion of sulfide reached above 99% with barely satisfactory selectivity (90.5%; the by-product was sulfone). We can conclude from the above results that the combination of {[Ni$_{0.5}$(1-vIM)$_2$]$_3$[Ni$_{0.5}$(1-vIM)H$_2$O]}$^{4+}$ and the [V$_4$O$_{12}$]$^{4-}$ cluster in **1** can produce the heterogeneous catalyst with excellent conversion and selectivity in the oxidation of methyl phenyl sulfide. Further, we speculate that the POVs parts in complexes **1**-**4** play an important role in improving the catalytic performance and the cation parts possibly contribute to enhance the selectivity toward sulfoxides in sulfoxidation process.

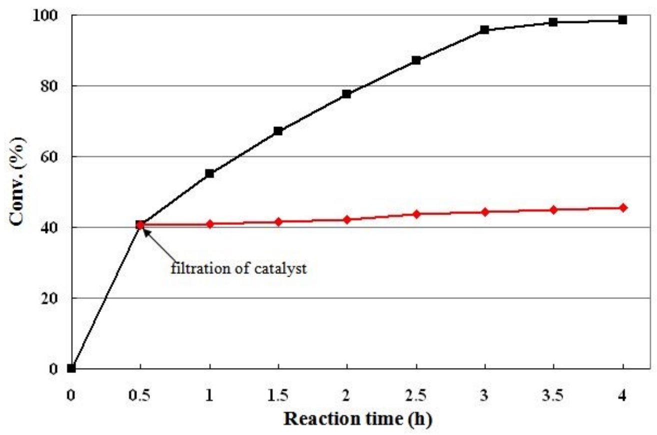

Figure 7. Kinetics of methyl phenyl sulfide sulfoxidation reaction catalyzed by **1** (black); **1** was filtrated from the reaction mixture after 0.5 h (red). Reaction conditions: sulfide (0.25 mmol), catalyst (8.75 µmol, 3.5 mol%), 30% aq H$_2$O$_2$ (0.3 mmol), 45 °C, ethanol (1 mL), 4 h.

To further elucidate the heterogeneity of complex **1** in the oxidative system, a hot leaching test was carried out. The solid catalyst **1** was filtrated off from the mixture after 0.5 h of reaction (conv. 40.5%; sele. toward sulfoxide 100%), and the filtrate was subsequently stirred at 45 °C for another 3.5 h. GC analysis of the resulting reaction mixture showed a negligible conversion after filtration (Figure 7). Atomic absorption analysis showed that there were no nickel and vanadium ions in the filtrate (S9 in the Supporting Information). All the above results collectively confirmed that the catalytic system is heterogeneous in nature. Furthermore, complex **1** can be easily separated by centrifugation after the completion of the reaction and can be reutilized at least 3 runs with remaining its activity and selectivity (methyl phenyl sulfide conversion of the third run remained above 96%, Figure 8). The IR spectrum (Figure S5) together with PXRD patterns (Figure S6) before and after catalysis demonstrated that the structure and the crystallinity of **1** was maintained during the reaction process.

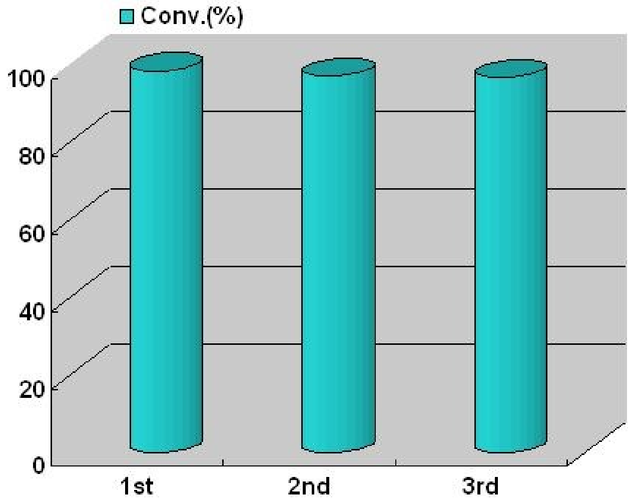

Figure 8. Recycle experiments of **1** in sulfoxidation reaction. Reaction conditions: methyl phenyl sulfide (5 mmol, 1 equiv.), **1** (175 µmol, 3.5 mol%), 30% aq H$_2$O$_2$ (5 mmol, 1.2 equiv.), 45 °C, ethanol (20 mL), 4 h.

The mild reaction conditions, excellent stability, and high yield for the transformation of methyl phenyl sulfide to methyl phenyl sulfoxide prompted us to extend the scope of **1** as heterogeneous catalyst for various sulfides. As shown in Table 2, the catalytic activity is remained when electron donor or acceptor groups with less steric hindrance are introduced in the monophenyl sulfides (Table 2, entries 2–4). Some typical dialkyl sulfides, such as *n*-butyl sulfide, and dimethyl sulfide were also investigated to examine the generality of **1** in sulfoxidation reactions. As shown in Table 2, entries 5–6, the optimized conditions could be also applicable to dialkyl sulfides, but the selectivity toward corresponding sulfoxide was slightly lower compared with that of monophenyl sulfides.

For the sulfur mustard abatement (Bis-(2-chloroethyl)sulfide, a chemical war agent), taken into account the high toxicity of real agent, 2-chloroethyl ethyl sulfide (CEES), was selected as the substrate to further study the catalytic activities of **1** in sulfoxidation system.[39] From Table 2, entry 7, we can see that satisfactory conversion and low selectivity toward 2-chloroethyl ethyl sulfoxide (CEESO) were obtained under the optimized conditions. To avoid peroxidation and obtain higher sulfoxide selectivity (2-chloroethyl ethyl sulfone (CEESO$_2$) is also more toxic),[40] we lowered the reaction temperature to 30 °C and prolonged the reaction time to 6h and prominent selectivity of CEESO was obtained (Table 2, entry 7).

View Article Online
DOI: 10.1039/D0DT03015E

Table 2. Selective oxidation of various sulfides to sulfoxides catalyzed by **1**.[a]

Entry	Substrates	Products	Conv. (%)	Sele. (%)[b]
1	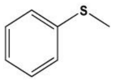	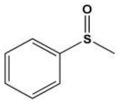	98.6	98.7
2	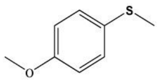	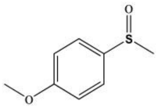	96.7	98.8
3	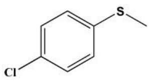	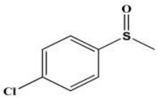	95.2	99.2
4	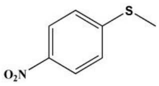	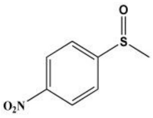	87.5	99.5
5	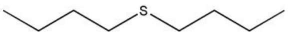	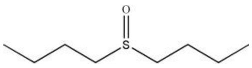	92.4	93.5
6	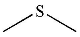	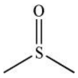	-[c]	83.7
7	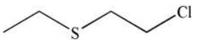	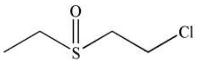	93.5 95.6[d]	82.5 94.5

[a]Reaction conditions: sulfide (1 mmol, 1 equiv.), **1** (35 µmol, 3.5 mol%), 30% aq H_2O_2 (1.2 mmol, 1.2 equiv.), 45 °C, ethanol (4 mL), 4 h. [b]Selectivity to corresponding sulfoxide. The byproduct is sulfone determined by GC-MS. [c]GC is not suitable for analyzing the compound with too low boiling point. [d]Temperature: 30 °C; Reaction time: 6 h.

It is rare to synthesize sulfoxide or sulfone by oxidizing sulfides using the same oxidant with high selectivity.[41] Given the high activity and selectivity of **1** for transformation of sulfides to sulfoxides, we further examined its utility of preparation of sulfones *via* oxidation of sulfides. The exploratory experiments started still using methyl phenyl sulfide as the model substrate. In order to improve the conversion of methyl phenyl sulfide and the selectivity toward methyl phenyl sulfone, increasing the amount of H_2O_2 and prolonging the reaction temperature is needed. At the same time, it is necessary to extend the reaction time. The high conversion of methyl phenyl sulfide (>99%) and selectivity toward corresponding sulfone (98.5%) were obtained under the optimized conditions. As shown in Table 3, entries 1-4, methyl phenyl sulfide and monophenyl sulfides several functional groups such as $-OCH_3$, -Cl, $-NO_2$, were oxidized to afford the corresponding sulfones in almost quantitative yields. Moreover, the dialkyl sulfides *n*-butyl sulfide and dimethyl sulfide worked perfect giving the sulfones with high conversion (97.4% for *n*-butyl sulfide) and selectivity (95.5% for *n*-butyl sulfone and 93.7% for dimethyl sulfone) (Table 3, entries 5-6).

Table 3. Selective oxidation of various sulfides to sulfones catalized by **1**.[a]

Entry	Substrates	Products	Conv. (%)	Sele. (%)[b]
1	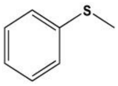	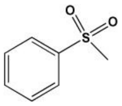	>99	98.5

View Article Online
DOI: 10.1039/D0DT03015E

2		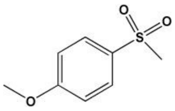	>99	98.2
3		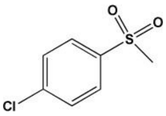	>99	97.2
4		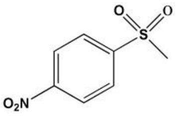	>99	96.5
5		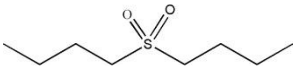	97.4	95.5
6		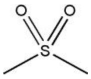	-[c]	93.7

[a]Reaction conditions: sulfide (1 mmol, 1 equiv.), **1** (35 μmol, 3.5 mol%), 30% aq H_2O_2 (3.0 mmol, 3 equiv.), 65 °C, ethanol (4 mL), 5 h. [b]Selectivity to corresponding sulfone. The byproduct is sulfoxide determined by GC-MS. [c]GC is not suitable for analyzing the compound with too low boiling point.

Experimental

Materials and methods

All chemicals were purchased from commercial suppliers and used without further purification. The metal content of the complexes **1**-**3** was measured by inductively coupled plasma (ICP) on an ICP-6000 analyzer. C, H, and N analyses of the neat complexes were conducted on Perkin-Elmer 240C elemental analyzer. The FT-IR spectra were recorded as KBr pellets in the range 4000–400 cm^{-1} on Nicolet 170 SXFT/IR spectrometer. The PXRD pattern was collected by using a Rigaku D/max-2550 diffractometer with Cuk_α radiation. The reaction products were analyzed by GC-MS (Agilent 7890A-5975C at an ionization voltage of 1200 V) and GC (Shimadzu GC-2014C with a FID detector equipped with an Rtx-1701 Sil capillary column).

Synthetic procedures

Synthesis of $[Ni_2(1\text{-vIM})_7H_2O][V_4O_{12}]\cdot H_2O$ (1): NH_4VO_3 (0.0939 g, 0.8 mmol) and $NiCl_2\cdot 6H_2O$ (0.1902 g, 0.8 mmol) were added to 10 mL water. Then 1-vIM (200 μL) was added. The resulting mixture was stirred for 1 h and then heated at 120 °C for 72 h under hydrothermal conditions. When cooling to room temperature, block pale blue crystals were obtained. Yield: 65% (based on NH_4VO_3). Anal. calcd. (%) (found) for $C_{35}H_{48}N_{14}Ni_2V_4O_{15}$: C, 34.29 (34.05); H, 3.95 (4.22); N, 15.99 (15.75); Ni, 9.57 (9.31); V, 16.62 (16.44). IR (KBr, cm^{-1}): 3416 (m), 3112 (m), 1650 (s), 1533 (w), 1498 (s), 1426 (w), 1381 (w), 1336 (m), 1279 (s), 1234 (s), 1092 (s), 1046 (w), 1005 (w), 930 (s), 797 (s), 655 (m), 594 (w), 513 (Ni-N, w).

Synthesis of $[Cu_2(1\text{-vIM})_8][V_4O_{12}]\cdot H_2O$ (2): The synthetic procedure was similar to that of complex **1** except that $CuCl_2\cdot 2H_2O$ (0.1363 g, 0.8 mmol) was used to replace $NiCl_2\cdot 6H_2O$. When cooling to room temperature, block dark purple crystals were obtained. Yield: 46% (based on NH_4VO_3). Anal. calcd. (%) (found) for $C_{40}H_{50}N_{16}Cu_2V_4O_{13}$: C, 37.13 (36.85); H, 3.90 (4.16); N, 17.32 (17.11); Cu, 9.82 (9.57); V, 15.75 (15.58). IR (KBr, cm^{-1}): 3417 (m), 3107 (m), 2924 (m), 1646 (s), 1503 (w), 1414 (w), 1380 (w), 1331 (w), 1286 (m), 1231 (m), 1104 (s), 1004 (w), 925 (s), 788 (s), 654 (m), 600 (w), 511 (Cu-N, w).

Synthesis of $[Co(1\text{-vIM})H_2O][VO_3]_2$ (3): When we try to improve the crystal quality of complex **4** by reducing the amount of $CoCl_2\cdot 6H_2O$, 1-vIM and adjustting the synthetic conditions as following: NH_4VO_3 (0.0939 g, 0.8 mmol) and $CoCl_2\cdot 6H_2O$ (0.0952 g, 0.4 mmol) were added to 10 mL water. Then 1-vIm (100 μL) was added. The resulting mixture was stirred for 1 h and then heated at 120 °C for 72 h. Fortunately, block pale blue crystals of **3** were obtained when cooling to room temperature. Yield: 54% (based on NH_4VO_3). Anal. calcd. (%) (found) for $C_5H_8N_2CoV_2O_7$: C, 16.28 (16.02); H, 2.19 (2.32); N, 7.59 (7.36); Co, 15.97 (15.75); V, 27.61 (27.39). IR (KBr, cm^{-1}): 3447 (m), 3122 (m), 1646 (w), 1616 (w), 1513 (w), 1404 (w), 1281 (w), 1242 (m), 1098 (m), 990 (m), 916 (s), 877 (m), 788 (s), 640 (s), 561 (Co-N, w).

Synthesis of $[Co_4(1\text{-vIM})_{14}][V_4O_{12}]_2\cdot 6H_2O$ (4): When we use the similar synthetic procedure to that of complex **1** except that $CoCl_2\cdot 6H_2O$ (0.1904 g, 0.8 mmol) was used to replace $NiCl_2\cdot 6H_2O$, block dark red crystals $[Co_4(1\text{-vIm})_{14}][V_4O_{12}]_2\cdot 6H_2O$ with poor quality were obtained as reported on our previous work.[27] Yield: 45% (based on NH_4VO_3). Anal. calcd. (%) (found) for $C_{70}H_{95}N_{28}Co_4V_8O_{30}$: C, 34.29 (34.02); H, 3.91 (4.11); N, 16.00 (15.82); Co, 9.61 (9.54); V, 16.62 (16.48). IR (KBr, cm^{-1}): 3443 (m), 3126 (m), 1648 (w), 1618 (w), 1515 (w), 1335 (w), 1286 (w), 1237 (m), 1110 (m), 983 (m), 958 (s), 920 (m), 882 (s), 778 (s), 647 (s), 564 (Co-N, w).

Crystallography

Crystallographic data for complexes **1**-**3** were conducted on a Bruker Smart APEX II CCD diffractometer with a graphite-monochromated Mo K*α* radiation (*λ* = 0.71073 Å). Absorption

View Article Online
DOI: 10.1039/D0DT03015E

corrections were applied using multi-scan technique with the SADABS program. The structures were solved and refined by SHELXS-2014 and SHELXL-2014 program packages.[42,43] Crystallographic data and structure refinement for **1**-**3** are summarized in Table 4. The crystallographic data have been deposited with the Cambridge Crystallographic Data Centre (CCDC) as entries 2021866 (**1**), 2021864 (**2**) and 2021865 (**3**).

Catalytic oxidative sulfoxidation process

For sulfoxides: substrate (1 mmol), catalyst (35 µmol, 3.5 mol %) and 30 % aq H_2O_2 (1.2 mmol) were stirred at 45 °C in ethanol (4 mL) for 4 h. **For sulfones:** substrate (1 mmol), catalyst (35 µmol, 3.5 mol %) and 30 % aq H_2O_2 (3.0 mmol) were stirred at 65 °C in ethanol (4 mL) for 5 h. The reaction mixture was heated slowly to the desired temperature in a Wattecs Parallel Reactor. After completion, the catalyst was simply retrieved by filtration and then washed with ethanol (ca. 3 × 5 mL). The resulting mixture was analyzed by GC-MS and GC.

Table 4. Crystallographic data for complexes **1**-**3**.

	1	**2**	**3**
Formula	$C_{35}H_{48}N_{14}Ni_2V_4O_{15}$	$C_{40}H_{50}N_{16}Cu_2V_4O_{13}$	$C_5H_8N_2CoV_2O_7$
M_r	1226.05	1293.80	368.94
Crystal system	Triclinic	Triclinic	Monoclinic
Space group	*P-1*	*P-1*	*P21/c*
T(K)	298(2)	298(2)	298(2)
a (Å)	12.6684(17)	10.8101(18)	12.057(3)
b (Å)	15.0479(19)	15.577(3)	5.8528(14)
c (Å)	15.759(2)	17.012(3)	15.556(4)
α (deg)	68.329(2)	84.690(3)	90
β (deg)	66.587(2)	76.443(3)	98.297(4)
γ (deg)	73.633(2)	74.492(3)	90
V (Å^3)	2529.6(6)	2682.1(8)	1086.2(4)
Z	2	2	4
$D_{calc.}$(g/cm^{-3})	1.610	1.602	2.256
F(000)	1248	1312	724
R_1 [$I>2\sigma(I)$]	0.0521	0.0574	0.0200
wR_2 [$I>2\sigma(I)$]	0.1422	0.1630	0.0568
R_1(all data)	0.0651	0.0799	0.0231
wR_2 (all data)	0.1537	0.1805	0.0586
GOOF	1.043	1.045	1.306
CCDC No.	2021866	2021864	2021865

Conclusions

In summary, we successfully prepared three new inorganic-organic hybrid POVs **1**-**3** by rationally controlling the hydrothermal synthetic conditions using 1-vIM as the N-donor ligand. The different final crystal structure of **3** compared with that of **1** and **2** indicate that the amount of 1-vIM is a crucial factor in the synthetic procedure of inorganic-organic hybrid POVs. All hybrid POVs show high heterogeneous catalytic activity and selectivity in the oxidation of sulfides to produce sulfoxides or sulfones respectively. Specifically, **1** show high activity and prominent selectivity toward CEESO in the CEES abatement reaction. Importantly, **1** can be simply recovered and recycled without losing its catalytic activity. The rational controlling synthesis of other hybrid POVs and the use of them in other catalytic reactions are in progress.

Conflicts of interest

There are no conflicts to declare.

Acknowledgements

DOI: 10.1039/D0DT03015E

We gratefully acknowledge support from the National Natural Science Foundation of China (No. 21871026, 21671019, 21871125), the Natural Science Foundation of Shandong Province (No. ZR2017LB002) and the Undergraduate Science and Technology Innovation Project of Shandong Provence (No. S201910453070).

Notes and references

1. (a) N. Mizuno, K. Yamaguchi and K. Kamata, *Coord. Chem. Rev.*, 2005, **249**, 1944; (b) D.-L. Long, E. Burkholder and L. Cronin, *Chem. Soc. Rev.,* 2007, **36**, 105; (c) S. S. Wang and G. Y. Yang, *Chem. Rev.*, 2015, **115**, 4893; (d) I. R. Weinstock, R. E. Schreiber and R. Neumann, *Chem. Rev.*, 2018, **118**, 2680; (e) J. X. Liu, X. B. Bang, Y. L. Li, S. L. Huang and G. Y. Yang, *Coord. Chem. Rev.*, 2020, **414**, 213260.
2. (a) Y. Hayashi, *Coord. Chem. Rev.*, 2011, **255**, 2270; (b) R. F. de Luis, J. L. Mesa, M. K. Urtiage, E. S. Larrea, T. Rojo and M. I. Arriortua, *Inorg. Chem.*, 2012, **51**, 2130; (c) K. Y. Monakhov, W. Bensch and P. Kögerler, *Chem. Soc. Rev.,* 2015, **44**, 8443; (d) H. M. Zhang, J. Yang, W. Q. Kan, Y. Y. Liu and J. F. Ma, *Cryst. Growth des.*, 2016, **16**, 265.
3. R. F. de Luis, J. L. Mesa, M. K. Urtiage, T. Rojo and M. I. Arriortua, *Eur. J. Inorg. Chem.*, 2009, 4786.
4. (a) J. Livage, *Coord. Chem. Rev.*, 1998, **178**, 999; (b) A. Muller, F. Peters, M. T. Pope and D. Gatteschi, *Chem. Rev.*, 1998, **98**, 239.
5. R. F. de Luis, J. Orive, E. S. Larrea, M. K. Urtiage and M. I. Arriortua, *CrystEngComm*, 2014, **16**, 10332.
6. E. S. Larrea, J. L. Mesa, J. L. Pizarro, M. Iglesias, T. Rojo and M. I. Arriortua, *Dalton Trans.*, 2011, **40**, 12690.
7. R. F. de Luis, M. K. Urtiage, J. L. Mesa, E. S. Larrea, T.Rojo and M. I. Arriortua, *Inorg Chem.*, 2013, **52**, 2615.
8. H. Lin and P. A. Maggard, *Inorg. Chem.*, 2008, **47**, 8044.
9. Y. Hu, F. Luo and F. Dong, *Chem. Commun.*, 2011, **47**, 761.
10. L. Luo and P. A. Maggard, *Cryst. Growth Des.*, 2013, **13**, 5282
11. B. B. Lu, J. Yang, Y. Y. Liu and J. F. Ma, *Inorg. Chem.*, 2017, **56**, 11710.
12. H. R. Tian, Z. Zhang, S. M. Liu, T. Y. Dang, X. H. Li, Y. Lu and S. X. Liu, *J. Mater. Chem. A*, 2020, **8**, 12398.
13. I. Fernández and N. Khiar, *Chem. Rev.*, 2003, **103**, 3651.
14. (a) A. M. Khenkin and R. Neumann, *J. Am. Chem. Soc.,* 2002, **124**, 4198; (b) F. Figueras, J. Palomeque, S. Loridant, C. Fèche, N. Essayem and G. Gelbard, *J. Catal.*, 2004, **226**, 25
15. R. Bentley, *Chem. Soc. Rev.,* 2005, **34**, 609.
16. K. Wang, Y. J. Niu, D. Y. Zhao, Y. X. Zhao, P. T. Ma, D. D. Zhang, J. P. Wang and J. Y. Niu, *Inorg. Chem.*, 2017, **56**, 14053.
17. M. D. Han, Y. J. Niu, R. Wan, Q. F. Xu, J. K. Lu, P. T. Ma, C. Zhang, J. Y. Niu and J. P. Wang, *Chem. - Eur. J.*, 2018, **43**, 11059.
18. R. Wan, P. P. He, Z. Liu, X. Y. Ma, P. T. Ma, V. Singh, C. Zhang, J. Y. Niu and J. P. Wang, *Chem. - Eur. J.*, 2020, **40**, 8760.
19. J. K. Lu, X. Y. Ma, V. Singh, Y. J. Zhang, P. T. Ma, C. Zhang, J. Y. Niu and J. P. Wang, *Dalton Trans.*, 2018, **47**, 5279.
20. S. Hussain, S. K. Bharadwaj, R. Pandey and M. K. Chaudhuri, *Eur. J. Org. Chem.*, 2009, **3319**.
21. N. Fukuda and T. Ikemoto, *J. Org. Chem.*, 2010, **75**, 4629.
22. K. Bahrami, M. M. Khodaei and M. S. Arabi, *J. Org. Chem.*, 2010, **75**, 6208.
23. X. Y. Shi, X. Y. Han, W. J. Ma, J. F. Wei, J. Li, Q. Zhang and Z. G. Chen, *J. Mol. Catal. A: Chem.*, 2011, **341**, 57.
24. Z. M. Wang, H. K. Lin, S. R. Zhu, T. F. Liu and Y. T. Chen, *J. Inorg. Biochem.*, 2002, **89**, 97.
25. T. M. Handyside, J. C. Lockhart, M. B. McDonnell and P. V. S. Rao, *J. Chem. Soc., Dalton Trans.*, 1982, 2331.
26. S. Jääskeläinen, I. O. Koshevoy, S. Suvanto, T. Ryhänen and P. Hirva, *New J. Chem.*, 2020, **44**, 12762.
27. (a) J. K. Li, X. Q. Huang, S. Yang, Y. Q. Xu and C. W. Hu, *Cryst. Growth Des.*, 2015, **15**, 1907; (b) J. K. Li, C. P. Wei, Y. Y. Wang, M. Zhang, X. R. Lv and C. W. Hu, *Inorg. Chem. Commun.*, 2018, **87**, 5.
28. J. K. Li, C. P. Wei, C. W. Hu, *Chin. Sci. Bull.*, 2018, **63**, 3342.
29. (a) X. Q. Huang, Y. Q. Qi, Y. X. Gu, S. W. Gong, G. D. Shen, Q. Li and J. K. Li, *Dalton Trans.*, 2020, **49**, 10970; (b) Y. H. Niu, S. Yang, J. K. Li, Y. Q. Xu and C. W. Hu, *Chin. Chem. Lett.*, 2016, **27**, 649.
30. (a) J. K. Li, X. Q. Huang, S. Yang, H. W. Ma, Y. N. Chi and C. W. Hu, *Inorg. Chem.*, 2015, **54**, 1454; (b) X. Q. Huang, J. K. Li, G. D. Shen, N. N. Xin, Z. G. Lin, Y. N. Chi, J. M. Dou, D. C. Li and C. W. Hu, *Dalton Trans.*, 2018, **47**, 726.
31. J. K. Li, R. T. Wu, J. X. Gong and C. W. Hu, *Journal of Liaocheng University: Natural Science Edition*, 2019, **32(3)**, 75.
32. W. Xu, F. Jiang, Y. Zhou, K. Xiong, L. Chen, M. Yang, R. Feng and M. Hong, *Dalton Trans.*, 2012, **41**, 7737.
33. Y. Hu, F. Luo and F. Dong, *Chem. Commun.*, 2011, **47**, 761.
34. S. J. Wu, X. H. Yang, J. F. Hu, H. W. Ma, Z. G. Lin and C. W. Hu, *CrystEngComm*, 2015, **17**, 1625.
35. A. K. Lyer, S. Roy, R. Haridasan, S. Sarkar and S. C. Peter, *Dalton Trans.*, 2014, **43**, 2153.
36. T. P. Vaid, S. P. Kelley and R. D. Rogers, *Dalton Trans.*, 2017, **46**, 8920.
37. O. Singh, N. Tyagi, M. M. Olmstead and K. Ghosh, *Dalton Trans.*, 2017, **46**, 14186.
38. C. X. Li, D. D. Zhong, X. Q. Huang, G. D. Shen, Q. Li, J. Y. Du, Q. L. Li, S. N. Wang, J. K. Li and J. M. Dou, *New J. Chem.*, 2019, **43**, 5813.
39. J. Dong, J. F. Hu, Y. N. Chi, Z. G. Lin, B. Zou, S. Yang, C. L. Hill and C. W. Hu, *Angew. Chem., Int. Ed.,* 2017, **56**, 4473.
40. J. K. Li, J. Dong, C. P. Wei, S. Yang, Y. N. Chi, Y. Q. Xu and C. W. Hu, *Inorg. Chem.*, 2017, **56**, 5748.
41. B. Yu, A. H. Liu, L. N. He, B. Li, Z. F. Diao and Y. N. Li, *Green Chem.*, 2012, **14**, 957.
42. G. M. Sheldrick, Phase Annealing in SHELX-90: Direct Methods for Larger Structures, *Acta Crystallogr., Sect. A: Found. Crystallogr.*, 1990, **46**, 46.
43. G. M. Sheldrick, A Short History of SHELX, *Acta Crystallogr., Sect. A: Found. Crystallogr.*, 2008, **64**, 112.

View Article Online
DOI: 10.1039/D0DT03015E

For Table of Contents only

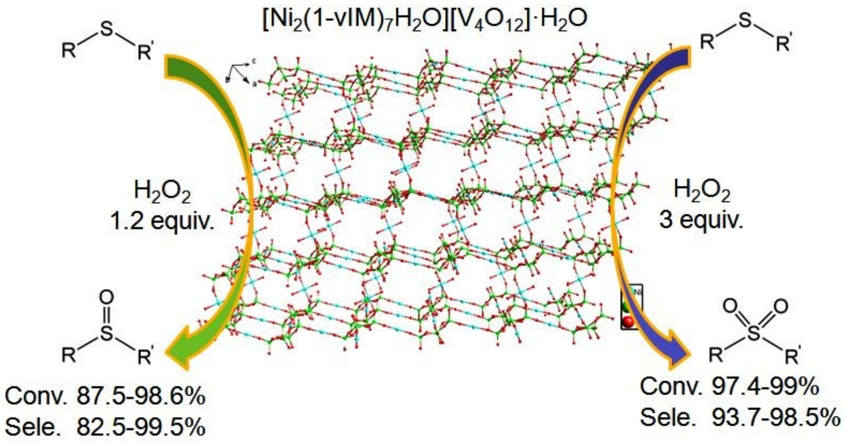

Three inorganic-organic hybrid polyoxovanadates $[Ni_2(1\text{-vIM})_7H_2O][V_4O_{12}]\cdot H_2O$ **(1)**, $[Cu_2(1\text{-vIM})_8][V_4O_{12}]\cdot H_2O$ **(2)** and $[Co(1\text{-vIM})H_2O][VO_3]_2$ **(3)** have been synthesized and fully characterized. Complex $[Ni_2(1\text{-vIM})_7H_2O][V_4O_{12}]\cdot H_2O$ (**1**), as a heterogeneous catalyst exhibit extraordinary catalytic performance (conv. of sulfides up to 98.6 %, sele. toward sulfoxides up to 99.5 %; conv. of sulfides up to >99 %, sele. up to 98.5 % for sulfones) in the sulfoxidation reactions using H_2O_2 as oxidant. Noticeably, complex **1** is stable in the catalytic recycling test and can be reused at least three times without losing its activity.